Process Biochemistry 128 (2023) 49–57

Contents lists available at ScienceDirect

Process Biochemistry

journal homepage: www.elsevier.com/locate/procbio

One-pot synthesis, characterisation and biological activities of gold nanoparticles prepared using aqueous seed extract of *Garcinia kola*

Scholastica O. Anadozie [a,b,*,1], Olusola B. Adewale [a,b], Nicole R.S. Sibuyi [c], Adewale O. Fadaka [c], Chinwe C. Isitua [d], Hajierah Davids [b], Saartjie Roux [b]

[a] Department of Biochemistry, Nanomedicine, Medicinal plant and Drug Toxicology Unit, Afe Babalola University, P.M.B 5454, Ado-Ekiti, Nigeria
[b] Department of Physiology, Nelson Mandela University, P.O Box 77000, Port Elizabeth, South Africa
[c] Department of Science and Innovation/Mintek Nanotechnology Innovation Centre, Biolabels Node, Department of Biotechnology, University of Western Cape, Private Bag X17, Bellville 7535, South Africa
[d] Department of Microbiology, Afe Babalola University, P.M.B 5454, Ado-Ekiti, Nigeria

ARTICLE INFO

Keywords:
Antioxidant
Anti-cancer
Biogenic
Garcinia kola
Gold nanoparticles

ABSTRACT

Recently, biogenic synthesis of gold nanoparticles (AuNPs) has become a focus area in cancer research owing to the eco-friendliness and cost effectiveness of the synthetic method. In this study, aqueous extract of *Garcinia kola* seed (AEGKs) was used for the bio-reduction of Au^{3+} to Au^{0}. The synthesised AEGKs-AuNPs was characterised by ultraviolet-visible (UV-Vis) spectroscopy, dynamic light scattering (DLS), high-resolution transmission electron microscopy (HRTEM) and Fourier transform-infrared (FT-IR) spectroscopy. The in vitro antioxidant activity of the AEGKs and AEGKs-AuNPs was evaluated using 2,2-diphenyl-1-picrylhydrazyl radical scavenging ability and ferric reducing antioxidant power assays. The AEGKs-AuNPs showed an absorption maximum at 512 nm, and the HRTEM images revealed mostly, spherical-shaped AuNPs in the size range of 2–17 nm. The FT-IR spectroscopy revealed that polyphenolic compounds and proteins were predominant, and responsible for the reduction and capping of the AuNPs. The AEGKs-AuNPs showed concentration dependent antioxidant activities, while dose-dependent in vitro anti-cancer activity of the AEGKs-AuNPs was demonstrated against lungs, prostrate, human cervical and human colon cancer cells, using the 3-(4,5-dimethylthiazol-2-yl)− 2,5-diphenyltetrazolium bromide tetrazolium reduction (MTT) assay. The antioxidant and anti-cancer activities of the AEGKs-AuNPs could be attributed to the presence of phytochemicals and physicochemical properties of the AuNPs.

1. Introduction

Cancer is a global health burden, with approximately 9.6 million deaths recorded in 2018 [1,2]. The increasing mortality rate associated with cancer calls for an urgent attention in the management of this disease [3]. The use of conventional treatment options, such as surgery, radiation and chemotherapy are limited by adverse effects including fatigue, anaemia, alopecia and thrombocytopenia [4,5].

Gold nanoparticles (AuNPs) have attracted great interest in biomedical applications because of its physicochemical properties such as tuneable size, shape, surface chemistry and biocompatibility [6]. Gold nanoparticles are used in bio-imaging, bio-labelling, bio-sensing, drug delivery, photodynamic therapy, as well as therapeutic agents for cancer [7–9]. Several approaches including physical, chemical, and biological methods are used in the synthesis of AuNPs. The physical and chemical methods of synthesising AuNPs makes use of toxic and hazardous chemicals, consumes higher energy, expensive and requires complex techniques [10,11]. The use of toxic chemicals affects biocompatibility of the AuNPs therefore, limiting its use in biomedical applications [12,13]. The biological approach on the other hand has greater advantage because of their dynamic nature which include products from natural sources, safety, and stability. In addition, this approach is economical and saves time as it requires a single-step bio-reduction process [14]. Another benefit of using biological synthesis is the ease to control size and shapes of AuNPs. These properties, enhance the retention and permeability effect of AuNPs at tumour site [15]. Biological (green)

* Corresponding author at: Department of Biochemistry, Nanomedicine, Medicinal plant and Drug Toxicology Unit, Afe Babalola University, P.M.B 5454, Ado-Ekiti, Nigeria.
E-mail addresses: anadozieso@abuad.edu.ng, scholanad2019@gmail.com (S.O. Anadozie).
[1] ORCID: 0000-0003-4118-4611

https://doi.org/10.1016/j.procbio.2023.02.010
Received 10 January 2021; Received in revised form 14 January 2023; Accepted 11 February 2023
Available online 13 February 2023

synthesis of AuNPs have recently been employed in drug delivery and cancer therapy because they produce stable and biocompatible AuNPs [16]. This method requires the use of microorganisms, animal metabolites, enzymes, plants or plant products to reduce inorganic metal ions to metal nanoparticle (NPs) [17–19]. Though microorganisms and enzymes have been exploited for the synthesis of AuNPs [17], plants have preference because phytochemicals have enhanced stability, do not require extensive purification, and lack of necessity in growing plants by employing technical culturing procedures to cultivate microorganisms [11]. Several medicinal plants have been used in the synthesis of AuNPs. These include *Nyctanthes arbortristis* [20], *Eucalyptus globulus* and *Rosmarinus offficinalis* [21], *Garcinia mangostana* [22], *Rosa hybrid* [23], *Salvia officinalis* [24] and *Plumeria alba* linn [25]. Biological activities such as antioxidant and anti-cancer properties of plant synthesised AuNPs have also been reported by several researchers. These include *Persea americana* [26], *Xylopia aethiopica* [11], *Sasa borealis* [27], *Lonicera japonica* [28], and *Achillea wilhelmssi* [29]. There are vast variety of plants with great biological properties that are yet to be explored for the synthesis of AuNPs.

Garcinia kola (*G. kola*), commonly known as bitter kola, is a flowering plant widely grown in the tropical regions of West and Central Africa [30]. It belongs to the plant family, Clusiaceae. Several parts of the *G. kola* plant (bark, root, leaf, seed and fruit) have been used in traditional medicine for managing various ailments such as bronchitis, colds, fever, laryngitis, cough, liver disease and bacterial infections [30–32]. The neuroprotective, hepatoprotective, anti-microbial, anti-inflammatory, anti-diabetic, antioxidant and chemo-preventive properties of *G. kola* have previously been reported [30,31,33–36]. The plant contains bioactive compounds such as tannins, flavonoids, alkaloids, proteins, phenolics and saponins [31]. Other compounds isolated from the seeds of *G. kola* includes kolaviron (a bioflavonoid), garcinoic acid, garcinal, benzophenone and kolanone [30]. Synthesis of metallic NPs using extracts of *G. kola* and its biological activities have also been reported [37,38]. To the best of our knowledge, no anti-cancer study has been reported using *G. kola* synthesised AuNPs. Therefore, the current study explored the synthesis of biogenic AuNPs using aqueous seed extract of *G. kola* and evaluate its in vitro antioxidant and anti-cancer properties.

2. Material and methods

2.1. Materials

Healthy, matured seeds of G. *kola* were purchased from Oja Bisi, Ado Ekiti, Ekiti State, Nigeria, West Africa. Tetrachloroauric acid ($HAuCl_4 0.3\ H_2O$), gallic acid, ascorbic acid, dimethyl sulfoxide (DMSO) and 5 ´-fluorouracil (5 ´FU) were purchased from Sigma-Aldrich, (St Louis, USA). 3-(4,5-dimethylthiazol-2-yl)− 2,5-diphenyltetrazolium bromide (MTT) and cell culture reagents were purchased from Thermo Fischer Scientific, (Massachusetts, USA) and Biowest (France), respectively. All chemicals used in this study were of analytical grade. The cancer cell lines; human non-small cell lung adenocarcinoma (A-549), human prostate cancer cells (PC3), human colorectal adenocarcinoma cells (HT-29) and human cervical cells (HeLa) used in this study were purchased from American Type Culture Collection (ATCC; Manassas, VA, USA).

2.2. Methods

2.2.1. Preparation of the aqueous seed extract of Garcinia kola

Garcinia kola seeds were peeled and washed thoroughly with Milli-Q water to remove impurities, and then drained of excess water. The seeds were cut into small pieces and air-dried at room temperature ($25 \pm 2\ ^\circ C$) in a dust-free environment for 7 days. The dried seeds were ground using an electric blender and stored in a desiccator at 4 °C until use. Aqueous seed extract of *G. kola* was achieved by adding 50 g of the powder into a beaker containing 500 mL Milli-Q water and incubated at 40 °C in a water bath for 24 h. The extract was filtered using Whatman no. 1 filter paper. The obtained extract was evaporated to dryness using rotary evaporator, and then lyophilised using a Sentry 2.0 Controller freeze-dryer (VirTis SP Scientific, UK). The lyophilised sample was stored at 4 °C until use.

2.3. Secondary metabolite screening of aqueous seed extract of Garcinia kola (AEGKs)

The presence of secondary metabolites in the AEGKs was screened using various methods as follows:

2.3.1. Flavonoids (Alkaline reagent test)

To 1 mL of AEGKs, 1 mL of 2% sodium hydroxide (NaOH) solution was added and mixed thoroughly until the colour turned yellow. A few drops of 1% hydrochloric acid (HCl) was added to the reaction mixture to obtain the final reaction colour [39].

2.3.2. Polyphenols (Ferric chloride ($FeCl_3$) test)

To 1 mL AEGKs, 3 drops 5% $FeCl_3$ was added, and the mixture was observed for a colour change [40].

2.3.3. Anthocyanidins

To 1 mL AEGKs, 1 mL 10% HCl was added and mixed gradually till a change in colour was observed [41].

2.3.4. Hydrolysable tannins

To 2 mL AEGKs, 1 mL potassium hydroxide was added, and the mixture was observed for a colour change [41].

2.3.5. Fats and oils

Fifty (50) µl AEGKs was dropped onto a filter paper Whatman no. 1 and allowed to dry for the presence of a ring stain, which indicates the presence of fats and oils [42].

2.3.6. Carbohydrates

To 1 mL AEGKs, 1 mL Fehling solution (equal volume of Fehling's A and Fehling's B reagents) was added to the test tube and boiled for 10 min to test the presence of carbohydrates [42].

2.3.7. Cardiac glycosides

To 1 mL AEGKs, 1 mL glacial acetic acid containing 2 drops 2% $FeCl_3$ solution was added. The mixture was transferred into another test tube and a few drops of concentrated sulphuric acid (H_2SO_4) was added and a colour change observed [41].

2.3.8. Alkaloids (Wagner's test)

To 2 mL of AEGKs, 1 mL 1% HCl was added and heated for about 20 min. A few drops of Wagner's reagent was added to the mixture to test the presence of alkaloids [40].

2.3.9. Saponin (Froth formation test)

To a test tube containing 2 mL AEGKs solution, 500 µl olive oil was added and mixed properly for 2 min for the formation of a stable froth to confirm the presence of saponin [40].

2.3.10. Anthraquinones

To 1 mL AEGKs, 500 µl 10% HCl was added and boiled for 4 min. The mixture was left at room temperature to cool. To the mixture, 500 µl chloroform and 500 µl 10% ammonia was added and vigorously shaken for the presence of anthraquinones [41].

2.3.11. Terpenoids

To 1 mL AEGKs, 1 mL chloroform was added and then evaporate to dryness by heating up to 100 °C in a water bath. Concentrated H_2SO_4

(500 μl) was added to the test tube and heated for another 2 min to test the presence of terpenoids [39].

2.3.12. Xanthoproteic test

To 2 mL AEGKs, 1 mL concentrated nitric acid was added and boil for 5 min. The solution was left to cool and 40% NaOH was added. The change in colour of the reaction mixture confirms the presence of xanthoproteic amino acids [41].

2.4. Biogenic synthesis of gold nanoparticles and their characterisation

2.4.1. Biogenic synthesis of gold nanoparticles

Aqueous extract of *G. kola* seeds gold nanoparticles (AEGKs-AuNPs) was performed by mixing varying concentrations of AEGKs (3.125 – 12.5 mg/mL) to 1 mM $HAuCl_4 0.3\ H_2O$ in a fixed volume ratio (1:4 v/v %) and temperature (25 and 50 °C). The 3.125 mg/mL concentration of AEGKs produced the most stabled AuNPs at 50 °C within 15 min and was used for subsequent synthesis. In brief, 40 mL of 3.125 mg/mL AEGKs was added to a beaker containing 160 mL of 1 mM $HAuCl_4 0.3\ H_2O$ and the reaction was allowed to proceed at 50 °C. The reaction mixture was observed for a colour change within the first 10 min. The heat was turned off and the solution stirred for another 5 min until a stable colour was observed. The synthesised AEGKs-AuNPs was washed with Milli-Q water twice to remove excess Au^{3+} solution and uncapped phytochemicals by means of centrifugation at 10000 x *g* for 20 min. The AEGKs-AuNP pellet was re-suspended in Milli-Q water and stored at 4 °C till required.

2.4.2. Characterisation of synthesised gold nanoparticles

The UV-Vis absorption measurement of the AEGKs-AuNPs was performed using NanoDrop 2000c spectrophotometer (Thermo Fischer Scientific, USA) [43], to determine the surface plasmon resonance (SPR) in a wavelength range of 300–800 nm. The hydrodynamic diameter and zeta potential measurements were performed using Zetasizer™ Nano ZS particle size analyser (Malvern Instruments Ltd, Worcestershire, UK) to determine the size, polydispersity index and surface charge of the AuNPs [44]. The core size and morphology of the AEGKs-AuNPs were obtained by HRTEM (JEOL. JEM-2100 LaB6, USA) at an accelerating voltage of 200 kV, while the crystalline nature of the AuNPs was determined using selected area electron diffraction (SAED) analysis. The HRTEM micrographs images were analysed using Image J Software Package (version 1.51). The FT-IR spectroscopic analysis was performed using the Perkin-Elmer spectrum one FT-IR spectrophotometer (Massachusetts, MA, USA) at a frequency of 4000–400 cm^{-1}, to determine the atomic vibrations in the organic coating and the functional groups on the surface of the AEGKs and AEGKs-AuNPs [45].

2.5. In vitro antioxidant activities of the AEGKs and AEGKs-AuNPs

2.5.1. In vitro antioxidants by 2,2-diphenyl-1-picrylhydrazyl radical scavenging assay

The 2,2-diphenyl-1-picrylhydrazyl (DPPH) radical scavenging ability of AEGKs and AEGKs-AuNPs was performed using modified method described by Adewale et al. [46]. Briefly, aliquots (3 μl) of various concentrations of AEGKs-AuNPs, AEGKs and quercetin (standard) (0.2 – 1 mg/mL) in Milli-Q water was added to 222 μl DPPH solution (0.1 mM in methanol). The reaction mixture for each sample was incubated at 37 °C in the dark for 30 min, and absorbance taken against methanol blank at 517 nm using a PowerWave HT microplate reader (Bio-Tek® Instruments, Inc., USA). The percentage inhibition of the DPPH radical scavenging activity was calculated as:

$$\%\ \text{inhibition} = \frac{\text{Abs}_{\text{control}} - \text{Abs}_{\text{test}}}{\text{Abs}_{\text{control}}} \times 100$$

Where Acontrol = absorbance of DPPH solution.

Table 1
Qualitative phytochemical screening of AEGKs.

Phytochemicals	AEGKs
Flavonoids	+ +
Polyphenols	+ +
Anthocyanidins	-
Hydrolysable tannins	-
Fats and oils	+ +
Carbohydrates	+ +
Cardiac glycosides	+ +
Alkaloids	+ +
Saponins	+ +
Anthraquinones	+
Terpenoids	+ +
xanthoproteic amino acid	+ +

Note: Presence of bioactive metabolites based on colour intensity. + + = present; + = moderately present; - = not detected.

Atest = absorbance of sample (AEGKs, AEGKs-AuNPs and standard) + DPPH solution.

The concentration that inhibits 50% (IC_{50}) of the scavenging activity of AEGKs and AEGKs-AuNPs was calculated from a linear regression analysis of concentration against % inhibition [46].

2.5.2. Ferric reducing antioxidant power

The ferric reducing antioxidant power (FRAP) of AEGKs and AEGKs-AuNPs was determined by the method of Benzie and Strain [47]. Briefly, 10 μl of various concentrations of AEGKs-AuNPs, AEGKs and ascorbic acid (0.2 – 1 mg/mL) in Milli-Q water was added to 300 μl freshly prepared FRAP reagent and incubated for 30 min at room temperature. Absorbance of the samples were read at 593 nm against reagent blank using a PowerWave HT microplate reader (Bio-Tek® Instruments, Inc., USA). Results were expressed as μmole ascorbic acid equivalent/litre (AAE/L).

2.6. Anticancer activity

2.6.1. Cell culture

The PC3, A549, HT-29 and Hela cells were cultured in Roswell Park Memorial Institute (RPMI) 1640, Dulbecco′s Modified Eagle′s Medium (DMEM) and DMEM-Ham's F12 media, respectively. All cell culture media were supplemented with 10% heat in-activated Foetal bovine serum (FBS) and 1% Penicillin-Streptomycin solution. The cells were grown under humidified condition with 5% CO_2 at 37 °C.

2.6.2. Cell viability assay

The effect of AEGKs-AuNPs on A549, PC3, HT-29 and HeLa was evaluated using MTT assay, as described by Mosmann [48], with minor modifications in seeding density and incubation time. The A549 and PC3 cells were seeded at 1×10^4 cells/100 μl/well, while HT-29 and HeLa cells were seeded at 1.5×10^4 cells/100 μl/well in a 96-well plate. The cells were treated with 6.25–100 μg/mL AEGKs-AuNPs and 100 μg/mL 5′-FU (positive control), respectively for 24 h [49]. The vehicle control (VC) used was 0.1% DMSO final well concentration. The purple formazan crystal was quantified by measuring absorbance at 570 nm and 630 nm (reference wavelength) using the PowerWave HT micro-plate reader (Bio-Tek® Instruments, Inc., USA) against media blank (without cells). The cell viability was calculated and expressed as percentage of treated cells against the VC. All tests were performed in triplicate of 3 individual experiments.

2.7. Statistical analysis

All results were expressed as mean ± standard deviation (SD), n = 3. One-way analysis of variance (ANOVA) was used for data analysis on GraphPad Prism 6.07, 2015. The significant difference between groups

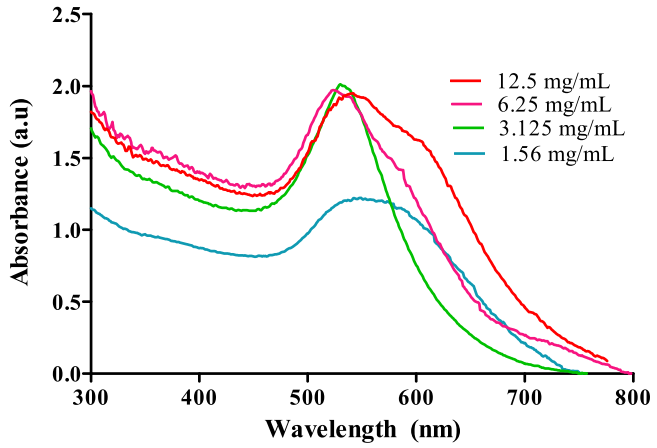

Fig. 1. Effect of concentration on the ultraviolet-visible absorption of AEGKs-AuNPs.

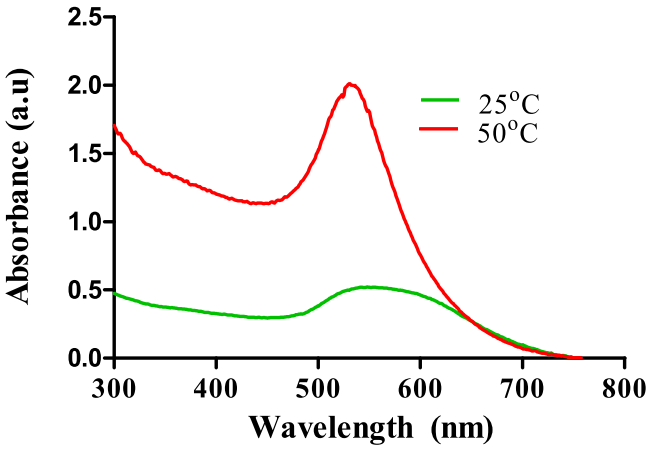

Fig. 2. Effect of temperature on the ultraviolet-visible absorption of AEGKs-AuNPs.

were determined using Tukey's post hoc multiple comparison test. The statistical significance was considered at $p < 0.05$ in all cases.

3. Results and discussion

3.1. Qualitative phytochemical screening of aqueous seed extract of Garcinia kola

Secondary metabolites screening of AEGKs showed the presence of flavonoids, polyphenols, fats and oils, carbohydrates, cardiac glycosides, alkaloids, saponins, terpenoids, and xanthoproteic amino acid as indicated in Table 1. Anthraquinone was moderately present while anthocyanidins and hydrolysable tannins were not detected. Although, previous study by Ukaoma et al. [31] reported the presence of tannins in ethanolic extract of *G. kola* seeds. The absence of tannins reported in this study could be because of the extraction method used. Secondary metabolites such as polyphenols, flavonoids and proteins are responsible for the reduction of gold salt to AuNPs [50]. These compounds were present in the secondary metabolites screening of AEGKs of this study (Table 1), and therefore, could be responsible for the reduction of AEGKs-AuNPs.

3.2. Biogenic synthesis and characterisation of gold nanoparticle

3.2.1. Biogenic synthesis of AEGKs-AuNPs

3.2.1.1. Effect of AEGKs concentration on the synthesis of AEGKs-AuNPs. The effect of various concentrations (3.125–12.5 mg/mL) of AEGKs for the synthesis of AEGKs-AuNPs was demonstrated by a single-step addition of AEGKs to 1 mM $HAuCl_4 0.3\ H_2O$ in a fixed volume ratio (1:4 v/v %). The varying concentrations of the AEGKs used in the present study produced different absorption peaks as demonstrated on the UV-Vis measurement of the synthesised AEGKs-AuNPs (Fig. 1). The AEGKs at 3.125 mg/mL produced a purple colour solution within 15 min, indicating the formation of AEGKs-AuNPs. The sharp intense absorption peak as observed in the present study could be relative to the excitation of the surface plasmon of the AuNPs [24]. The broad absorption peaks of the AEGKs-AuNPs obtained at 1.56, 6.25 and 12.5 mg/mL AEGKs suggest that the concentrations of the plant extract produced larger AuNPs which may agglomerate. The findings of this study is in agreement with the previous reported studies where higher concentration of biogenic AuNPs resulted in NPs agglomeration [51,52]. Since the concentration of AEGKs at 3.125 mg/mL gave the most stabled AEGKs-AuNPs it was adopted for larger scale synthesis, characterisation, and other bioassays.

3.2.1.2. Effect of temperature on the AEGKs-AuNPs formation. Temperature is crucial in the biogenic synthesis of AuNPs because of its effect in the production of rapid and small-sized AuNPs. Optimisation of temperature (25 and 50 °C) for the synthesis of AEGKs-AuNPs was performed in the present study. At 25 °C, a moderate reaction rate was observed for the synthesised AuNPs. The produced AuNPs was unstable and showed a broad absorption peak on the UV-Vis measurement (Fig. 2). A maximum reaction was observed at 50 °C with the appearance of a purple colour. In addition, a sharp absorption peak was produced (Fig. 2), suggesting a stable and small-sized AEGKs-AuNPs. A study by Ghosh et al. [53] support our findings that higher temperature enhances the rate of reaction during the synthesis of AuNPs, and also produces rapid and small-sized AuNPs.

3.2.2. Characterisation AEGKs-AuNPs

3.2.2.1. UV-Vis spectroscopy of AEGKs-AuNPs. The UV-Vis analysis of AEGKs-AuNPs showed a broad optical absorption maximum at 530 nm (Fig. 3A). This falls within the SPR of AuNPs (500–600 nm) and thus confirms the formation of AuNPs [50]. The synthesis occurred using Au solution, and AEGKs as the reducing and stabilizing agent in the absence of toxic chemical agents. The phytochemicals in the AEGKs which is suspected to be mainly polyphenolic compounds and proteins as shown in Table 1 could be responsible for the reduction of Au^{3+} to Au^0. Similar findings has been reported for *Catharanthus roseus* and *Carica papaya*, *Achillea wilhelmsii* and *Lonicera japonica* that the inherent phytochemicals were suggested to be responsible for the reduction and stabilisation of the AuNPs formed [28,29,54].

3.2.2.2. Dynamic light scattering and zeta potential measurement. Dynamic light scattering and zeta potential measurements were performed to determine the size distribution, polydispersity index (PDI) and surface charge of the AEGKs-AuNPs in aqueous medium. The AEGKs-AuNPs had a hydrodynamic diameter of 32.27 ± 0.12 nm (Fig. 3B) and a PDI of 0.296. Nanoparticles with a PDI value above 0.7 have a broad particle size distribution and are unstable in solution [55]. The PDI of AEGKs-AuNPs showed uniformity of the AuNPs and how well they are dispersed in the aqueous medium. It could also be that the sizes of the AEGKs-AuNPs are in close range. These findings were further confirmed by the result of the HRTEM (Fig. 4A).

Zeta potential (*ZP*) measures the surface potential and possible interaction of the AuNPs within the cells. In the present study, the *ZP* of AEGKs-AuNPs was -30.9 ± 0.42 mV (Fig. 3C), the high anionic *ZP* value results in an increased light scattering which can be linked to the small size of the AuNPs [56]. The negative (-) *ZP* value might be due to the presence of phytochemicals with a carboxylic functional groups on the surface of the AuNPs [57], and provides strong repulsion forces

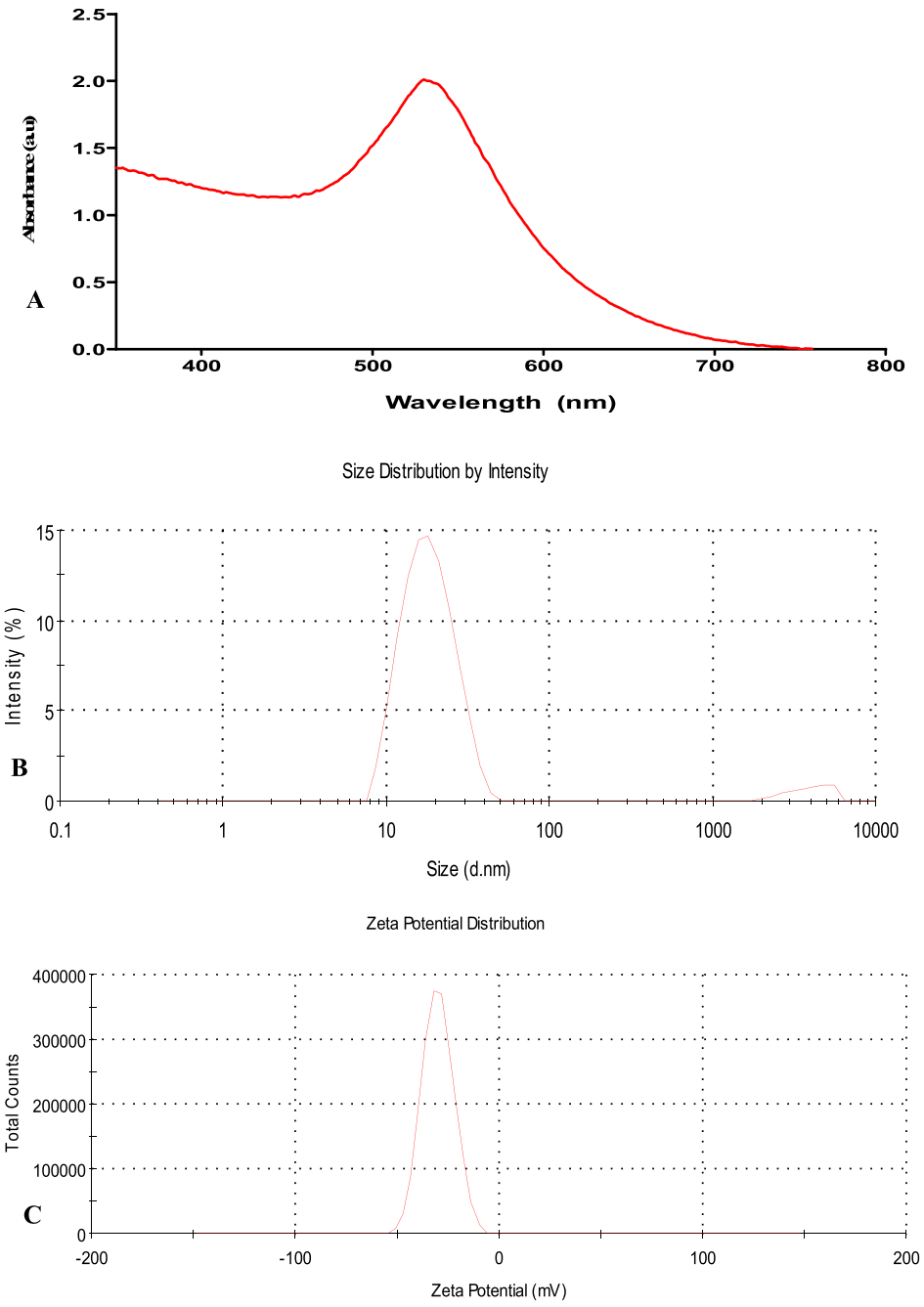

Fig. 3. Ultraviolet-visible absorption spectrum of AEGKs-AuNPs (A), size distribution (B) and zeta potential of AEGKs-AuNPs (C).

between the AuNPs thereby preventing NPs agglomeration in solution [15,58].

3.2.3. *High resolution transmission microscopy of AEGKs-AuNPs*

The size distribution, morphology, and crystallinity of the AuNPs are shown in Fig. 4A-C. The AEGKs produced mostly spherical-shaped AuNPs, with a core size ranging between 2 and 17 nm. The particle size in HRTEM differ from that of DLS because DLS measures NPs size alongside the surface layer surrounding the particle in medium, while the HRTEM measures only the metal core size [55]. The arrow in Fig. 4B indicates the presence of phytochemicals in the AEGKs around the gold core.

The crystalline nature of AEGKs-AuNPs was confirmed by the SAED ring pattern (Fig. 4C), with five bright circular rings corresponding to the Bragg's reflection lattice planes (111), (200), (220), (311) and (222) scattering of face-centred cubic (fcc) of Au (JCPDS no. 04–0784) [59, 60]. Similar fcc AuNPs patterns has been reported for *B. javanica Blume* leaves extract synthesized AuNPs [61].

3.2.4. *Fourier transmission-infrared spectroscopy*

The FT-IR spectra analysis revealed the functional groups in the AEGKs that are involved in the bio-reduction of Au^{3+} to Au^{0}. The characteristic absorption bands of the different functional groups present in AEGKs and AEGKs-AuNPs are shown in Table 2, Supplementary 1. Some of the absorption peaks displayed similarity for both AEGKs and AEGKs-AuNPs, suggesting the presence of the same functional groups, and phytochemical involved in the reduction and capping of the AuNPs.

The presence of functional groups such as O-H, N-H, C═O and C═C indicates that the phytochemicals responsible for the reduction and capping of the AuNPs are compounds containing flavonoids, alkaloids

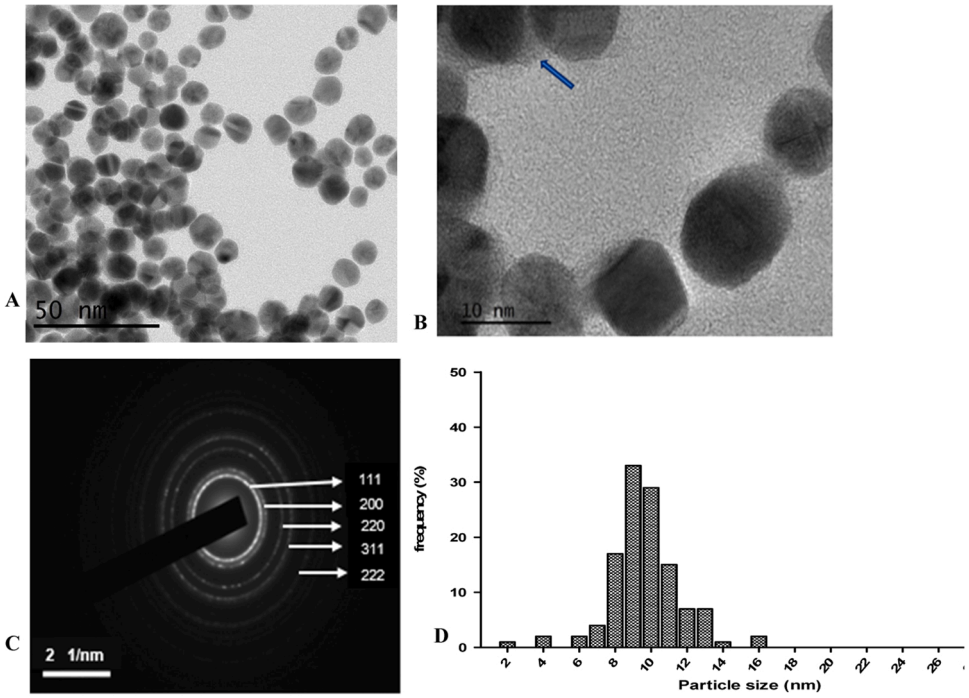

Fig. 4. High-resolution transmission electron microscopy of AuNPs at 50 nm (A) and 10 nm (B) scale bars. Selected area electron diffraction pattern indicating the lattice planes of the AuNPs (C), and size distribution of AEGKs-AuNPs (D).

Table 2
Fourier transmission infrared spectroscopic analysis of AEGKs and AEGKs-AuNPs showing shift in absorption position and functional groups responsible for the reduction and capping of AuNPs.

AEGKs absorption bands (cm^{-1})	AEGKs-AuNPs absorption bands (cm^{-1})	Shift in position (cm^{-1})	Functional groups present in samples
3311.46	3332.15	+ 20.69	-OH (phenol); N-H stretching amine
2893.17	2785.18	-107.99	
ND	2278.83	-	H–C═O; C–H stretch aldehydes
2170.48	2169.93	-0.55	C═C stretch
1964.98	1876.05	-0.51	C═C
1635.13	1637.25	+ 2.12	C═O anhydrides
1492.83	1492.36	-0.47	-C═C- stretch alkenes
1394.29	1371.38	-22.91	-C═C- stretch alkynes
1051.90	1031.78	-20.12	C-H methyl rock alkanes
923.28	865.10	-58.18	C-O stretch
699.81	ND	-	C-H bending

Shift in absorption band were calculated by subtracting the peak position in AEGKs-AuNPs from the peak position in AEGKs.
AEGKs - aqueous seed extract of *Garcinia kola;* AuNPs - gold nanoparticles; ND - not detected.

and terpenoids [50]. The N-H and C-H groups suggests the presence of protein on the surface of the AuNPs, which is responsible for the capping of the NPs, and prevents agglomeration [15]. A shift in absorption peaks of the AEGKs-AuNPs and AEGKs from 3332.15 to 3311.46 cm^{-1}, and from 1637.25 to 1635.13 cm^{-1} suggests that O-H (polyphenolic compounds) and N-H (proteins) are the main functional groups responsible for the reduction of Au^{3+} to AuNPs. The findings of the present study agrees with a study by Dzimitrowicz et al. [62] where a shift in absorption peak was noted in AuNPs synthesised from *Lamiaceae* plants when compared with the plant extract.

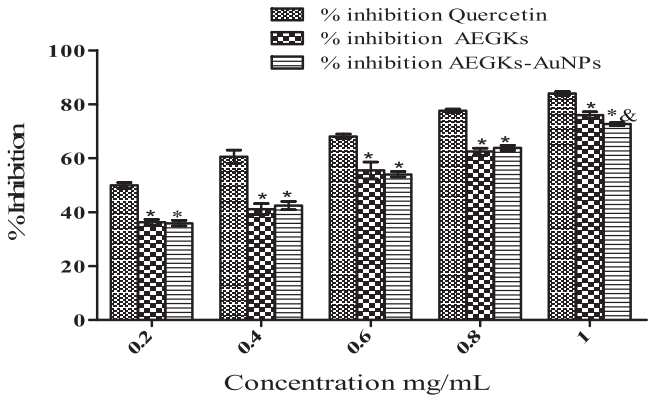

Fig. 5. 2,2-diphenyl-1-picrylhydrazyl radical scavenging activity of aqueous seed extract of *G. kola* (AEGKs) and the corresponding gold nanoparticles (AEGKs-AuNPs).

3.3. *In vitro antioxidant and reducing properties assays*

3.3.1. *Antioxidant activity and reducing power of AEGKs and AEGKs-AuNPs*

The antioxidant activities and reducing power of both AEGKs and AEGKs-AuNPs were investigated using DPPH and FRAP assays.

3.3.1.1. 2,2-diphenyl-1-picrylhydrazyl radical scavenging activity. The *G. kola* has been reported to possess good antioxidant properties [30]. Since antioxidants are responsible for the reduction of AuNPs [63], this study therefore evaluated the antioxidant capacity of AEGKs and its synthesised AEGKs-AuNPs. The DPPH free radical scavenging activity of the samples showed a dose-dependent response (Fig. 5). No significant difference ($p > 0.05$) was noted in the radical scavenging activity of AEGKs-AuNPs when compared to the AEGKs, except at 1 mg/mL, where a significant ($p < 0.05$) difference in the radical scavenging activity was seen. This suggests that the antioxidant activity of the AEGKs-AuNPs was

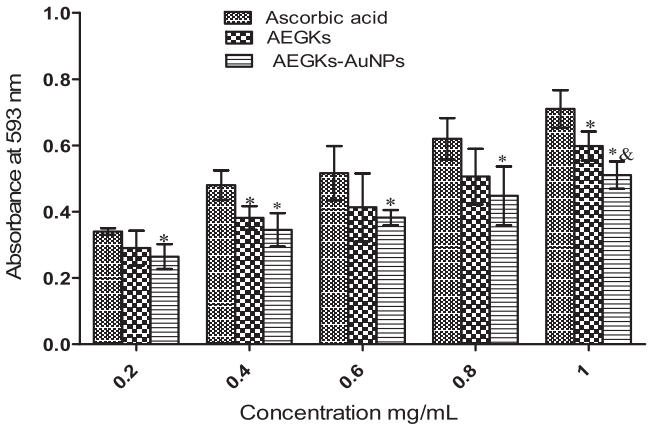

Fig. 6. Ferric reducing antioxidant power (FRAP) of aqueous seed extract of *G. kola* (AEGKs) and corresponding gold nanoparticles (AEGKs-AuNPs).

retained after the synthesis. It further validates the FT-IR spectra analysis (Table 2), where the same functional groups were seen in both AEGKs and AEGK-AuNPs, therefore, suggesting the presence of similar phytochemicals. Similar findings was reported in the study by Nakkala et al. [64], where *Piper longum* fruit extract and its synthesised AuNPs showed good DPPH radical scavenging activity. The positive control (Quercetin) had higher scavenging potency with an IC_{50} value of 0.18 mg/mL, while AEGKs and AEGKs-AuNPs had IC_{50} values of 0.51 and 0.52 mg/mL, respectively.

3.3.1.2. Ferric reducing antioxidant power. The FRAP properties of the samples increased in a concentration dependent manner (Fig. 6). Ascorbic acid was significantly ($p < 0.05$) higher in the FRAP activity than AEGKs and AEGKs-AuNPs, except for 0.2, 0.6 and 0.8 mg/mL AEGKs, where no significant difference ($p > 0.05$) was observed in the FRAP activity when compared to the ascorbic acid, therefore, it can be suggested that AEGKs has good antioxidant activity. A significant ($p < 0.05$) difference in the FRAP activity was noted in the 1 mg/mL AEGKs-AuNPs when compared to AEGKs. The findings of this study, therefore, suggest the involvement of phytochemicals in the reduction and capping of the AEGKs-AuNPs.

3.4. Anti-cancer activity of AEGKs-AuNPs

The anti-cancer potency of AEGKs-AuNPs was demonstrated on cancer (A549, PC3, Hela and HT-29) cells after 24 h treatment. As revealed in Fig. 7, the AEGKs-AuNPs was cytotoxic to all cell lines used in this study and reduced their viability in a concentration dependent manner. The Hela cells were the most susceptible to the effects of the AuNPs from the lower concentration (6.25 μg/mL), followed by A549 and HT-29 cells (12.5 μg/mL). Significant effect of the AuNPs on PC3 cells occurred at higher concentrations (< 50 μg/mL). At 100 μg/mL, both AEGKs-AuNPs and standard anti-cancer drug (5′-FU) were comparable in terms of susceptibility to cell lines tested. Previous study by Olatunde et al. [65] reported that the essential oils from *G. kola* seeds were effective against A549 and HeLa cells at 8.3 mg/mL with cell viability of 98.0% and 94.7%, respectively. However, in our study, it was noted that the cell viability of AEGKs-AuNPs, at 6.25 and 100 μg/mL, against A549 were 91.2% and 9.7%, respectively, and 67.1% and 19.3%, respectively for HeLa cells. It could be noted based on these two studies that AEGKs-AuNPs possess more cytotoxic effect than the essential oils. This may be attributed to the physicochemical properties (size, shape, and surface chemistry) of the delivery system (AuNPs), as well as the stability of the AuNPs [29,66]. The IC_{50} values of AEGKs-AuNPs for the four cancer cell lines are demonstrated in Table 3. The highest inhibitory activity of AEGKs-AuNPs was observed in HeLa cells with an IC_{50} value of 10.72 μg /mL, indicating that the AEGKs-AuNPs were more cytotoxic against HeLa cells, followed by A549, HT-29 and PC3. The high sensitivity and cytotoxicity of AEGKs-AuNPs against these four cancer cell lines therefore suggests the possible role of the AEGKs-AuNPs in cancer therapy.

Table 3
Summary of IC_{50} values calculated for treated A549, PC3, HeLa and HT-29 cells.

Treatments (IC_{50})	A549 cells	PC3 cells	HeLa cells	HT-29 cells
AEGKs-AuNPs	24.62 ± 0.41 μg /mL	69.05 ± 0.01 μg /mL	10.72 ± 0.22 μg /mL	41.85 ± 0.08 μg /mL

AEGKs - aqueous seed extract of Garcinia kola; AuNPs - gold nanoparticles

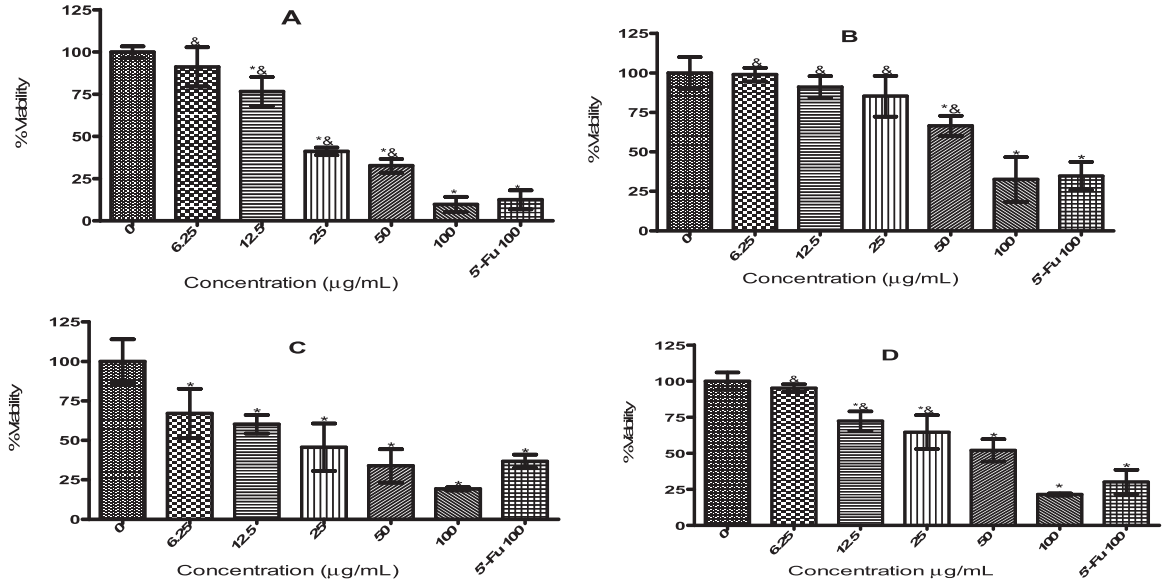

Fig. 7. Anti-cancer activity of AEGKs-AuNPs against different cancer cells.; A549 (A), PC3(B), HeLa(C), HT-29 (D) were treated with increasing concentrations of AEGKs-AuNPs for 24 h, cell viability was assessed using MTT assay.

4. Conclusion

The present study reports the one-pot synthesis of AuNPs using aqueous seed extract of *G. kola*, and its biological activities. *Garcinia kola* was selected based on its previously reported medicinal properties. The AEGKs served as reducing and capping agents in the synthesis of AuNPs. The FT-IR results showed that polyphenolic compounds such as flavonoids, polyphenol and terpenoids were responsible for the reduction of AuNPs. The antioxidant activity of the AEGKs-AuNPs suggests that phytochemicals could be involved in the synthesis of the AuNPs, and therefore, responsible for their enhanced anti-cancer activities. The cytotoxicity of the AEGKs-AuNPs on different cancer cells can be attributed to the physicochemical properties of the AuNPs which includes nano-size, morphology, and surface chemistry. Further studies are underway to evaluate the cellular uptake and mechanism of cell death using the AEGKs-AuNPs.

Acknowledgments

The authors wish to acknowledge Prof. Mervin Meyer for gifting with A549 and HeLa cell lines used in this study. The authors wish to thank Dr. Arno Janse van Vuuren for HRTEM image analysis at the Department of Physics Nelson Mandela University.

Conflict of interest

The authors declare no conflict of interest.

Author contributions

S.O.A., H.D., and S.R. conceived and designed the experiments, S.O.A., and O.B.A. drafted the manuscript, N.R.S.S., H.D., and S.R. reviewed the manuscript, FOA and CCI coordinated the data analysis. All authors contributed significantly to this manuscript, read, and gave final approval of the version to be published.

Appendix A. Supporting information

Supplementary data associated with this article can be found in the online version at doi:10.1016/j.procbio.2023.02.010.

References

[1] F. Bray, J. Ferlay, I. Soerjomataram, R.L. Siegel, L.A. Torre, A. Jemal, Global cancer statistics 2018: GLOBOCAN estimates of incidence and mortality worldwide for 36 cancers in 185 countries, CA: *A Cancer J. Clin.*, 68 (2018) 394–424.
[2] W.H.O., Latest global cancer data: Cancer burden rises to 18.1 million new cases and 9.6 million cancer deaths in 2018, in, Geneva, WHO Press, 2018.
[3] H. Mohandas, S.K. Jaganathan, M.P. Mani, M. Ayyar, G.R. Thevi, Cancer-related fatigue treatment: an overview, J. Cancer Res. Ther. 13 (2017) 916.
[4] C. Pucci, C. Martinelli, G. Ciofani, Innovative approaches for cancer treatment: current perspectives and new challenges, Ecancermedicalscience 13 (2019), 961-961.
[5] S. Senapati, A.K. Mahanta, S. Kumar, P. Maiti, Controlled drug delivery vehicles for cancer treatment and their performance, Signal Transduct. Target. Ther. 3 (2018) 1–19.
[6] W. Li, Z. Cao, R. Liu, L. Liu, H. Li, X. Li, Y. Chen, C. Lu, Y. Liu, AuNPs as an important inorganic nanoparticle applied in drug carrier systems, Artif. Cells, Nanomed., Biotechnol. 47 (2019) 4222–4233.
[7] A. Khan, R. Rashid, G. Murtaza, A. Zahra, Gold nanoparticles: synthesis and applications in drug delivery, Trop. J. Pharm. Res. 13 (2014) 1169–1177.
[8] A. Sett, M. Gadewar, P. Sharma, M. Deka, U. Bora, Green synthesis of gold nanoparticles using aqueous extract of *Dillenia indica*, Adv. Nat. Sci.: Nanosci. Nanotechnol. 7 (2016), 025005.
[9] S. Suvarna, U. Das, K. Sunil, S. Mishra, M. Sudarshan, K.D. Saha, S. Dey, A. Chakraborty, Y. Narayana, Synthesis of a novel glucose capped gold nanoparticle as a better theranostic candidate, PloS One 12 (2017), e0178202.
[10] S.O. Anadozie, O.B. Adewale, A.O. Fadaka, O.B. Afolabi, S. Roux, Synthesis of gold nanoparticles using extract of *Carica papaya* fruit: evaluation of its antioxidant properties and effect on colorectal and breast cancer cells, Biocatal. Agric. Biotechnol. 42 (2022), 102348.
[11] S.O. Anadozie, O.B. Adewale, M. Meyer, H. Davids, S. Roux, *In vitro* anti-oxidant and cytotoxic activities of gold nanoparticles synthesized from an aqueous extract of the *Xylopia aethiopica* fruit, Nanotechnology (2021).
[12] H. Bagur, C.C. Poojari, G. Melappa, R. Rangappa, N. Chandrasekhar, P. Somu, Biogenically synthesized silver nanoparticles using endophyte fungal extract of ocimum tenuiflorum and evaluation of biomedical properties, J. Clust. Sci. 31 (2020) 1241–1255.
[13] M. Dhayalan, M.I.J. Denison, M. Ayyar, N.N. Gandhi, K. Krishnan, B. Abdulhadi, Biogenic synthesis, characterization of gold and silver nanoparticles from *Coleus forskohlii* and their clinical importance, J. Photochem. Photobiol. B: Biol. 183 (2018) 251–257.
[14] I. Hammami, N.M. Alabdallah, A.A. jomaa, M. kamoun, Gold nanoparticles: synthesis properties and applications, J. King Saud. Univ. - Sci. 33 (2021), 101560.
[15] K.X. Lee, K. Shameli, Y.P. Yew, S.-Y. Teow, H. Jahangirian, R. Rafiee-Moghaddam, T.J. Webster, Recent developments in the facile bio-synthesis of gold nanoparticles (AuNPs) and their biomedical applications, Int. J. Nanomed. 15 (2020) 275.
[16] A.C. Barai, K. Paul, A. Dey, S. Manna, S. Roy, B.G. Bag, C. Mukhopadhyay, Green synthesis of *Nerium oleander*-conjugated gold nanoparticles and study of its in vitro anticancer activity on MCF-7 cell lines and catalytic activity, Nano Converg. 5 (2018), 10-10.
[17] I.C. Oladipo, A. Lateef, J.A. Elegbede, M.A. Azeez, T.B. Asafa, T.A. Yekeen, A. Akinboro, E.B. Gueguim-Kana, L.S. Beukes, T.O. Oluyide, O.R. Atanda, Enterococcus species for the one-pot biofabrication of gold nanoparticles: characterization and nanobiotechnological applications, J. Photochem. Photobiol. B: Biol. 173 (2017) 250–257.
[18] A. Lateef, S.A. Ojo, J.A. Elegbede, The emerging roles of arthropods and their metabolites in the green synthesis of metallic nanoparticles, Nanotechnol. Rev. 5 (2016) 601–622.
[19] A. Singh, P.K. Gautam, A. Verma, V. Singh, P.M. Shivapriya, S. Shivalkar, A. K. Sahoo, S.K. Samanta, Green synthesis of metallic nanoparticles as effective alternatives to treat antibiotics resistant bacterial infections: a review, Biotechnol. Rep. 25 (2020), e00427.
[20] R.K. Das, N. Gogoi, U. Bora, Green synthesis of gold nanoparticles using Nyctanthes arbortristis flower extract, *Bioprocess Biosyst. Eng.*, 34 (2011) 615–619.
[21] A. Dzimitrowicz, S. Berent, A. Motyka, P. Jamroz, K. Kurcbach, W. Sledz, P. Pohl, Comparison of the characteristics of gold nanoparticles synthesized using aqueous plant extracts and natural plant essential oils of *Eucalyptus globulus* and *Rosmarinus officinalis*, Arab. J. Chem. 12 (2019) 4795–4805.
[22] J.S. Park, E.-Y. Ahn, Y. Park, Asymmetric dumbbell-shaped silver nanoparticles and spherical gold nanoparticles green-synthesized by mangosteen (*Garcinia mangostana*) pericarp waste extracts, Int. J. Nanomed. 12 (2017) 6895.
[23] R. Mythili, T. Selvankumar, P. Srinivasan, A. Sengottaiyan, J. Sabastinraj, F. Ameen, A. Al-Sabri, S. Kamala-Kannan, M. Govarthanan, H. Kim, Biogenic synthesis, characterization and antibacterial activity of gold nanoparticles synthesised from vegetable waste, J. Mol. Liq. 262 (2018) 318–321.
[24] M.H. Oueslati, L. Ben Tahar, A.H. Harrath, Synthesis of ultra-small gold nanoparticles by polyphenol extracted from *Salvia officinalis* and efficiency for catalytic reduction of p-nitrophenol and methylene blue, Green. Chem. Lett. Rev. 13 (2020) 18–26.
[25] R. Mata, A. Bhaskaran, S.R. Sadras, Green-synthesized gold nanoparticles from *Plumeria alba* flower extract to augment catalytic degradation of organic dyes and inhibit bacterial growth, Particuology 24 (2016) 78–86.
[26] A.E. Adebayo, A.M. Oke, A. Lateef, A.A. Oyatokun, O.D. Abisoye, I.P. Adiji, D. O. Fagbenro, T.V. Amusan, J.A. Badmus, T.B. Asafa, L.S. Beukes, E.B. Gueguim-Kana, S.H. Abbas, Biosynthesis of silver, gold and silver–gold alloy nanoparticles using *Persea americana* fruit peel aqueous extract for their biomedical properties, Nanotechnol. Environ. Eng. 4 (2019) 13.
[27] M.P. Patil, X. Jin, N.C. Simeon, J. Palma, D. Kim, D. Ngabire, N.-H. Kim, N.H. Tarte, G.-D. Kim, Anticancer activity of *Sasa borealis* leaf extract-mediated gold nanoparticles, Artif. Cells, Nanomed., Biotechnol. 46 (2018) 82–88.
[28] M.P. Patil, E. Bayaraa, P. Subedi, L.L.A. Piad, N.H. Tarte, G.-D. Kim, Biogenic synthesis, characterization of gold nanoparticles using Lonicera japonica and their anticancer activity on HeLa cells, J. Drug Deliv. Sci. Technol. 51 (2019) 83–90.
[29] M. Asariha, A. Chahardoli, N. Karimi, M. Gholamhosseinpour, A. Khoshroo, H. Nemati, Y. Shokoohinia, A. Fattahi, Green synthesis and structural characterization of gold nanoparticles from *Achillea wilhelmsii* leaf infusion and in vitro evaluation, Bull. Mater. Sci. 43 (2020) 57.
[30] E.O. Farombi, O. Owoeye, Antioxidative and chemopreventive properties of Vernonia amygdalina and Garcinia biflavonoid, Int. J. Environ. Res. Public Health 8 (2011) 2533–2555.
[31] A. Ukaoma, V. Ukaoma, R. Okechukwu, M. Iwuagwu, Phytochemical screening and antibacterial properties of Garcinia kola, J. Phytopharm. 2 (2013) 34–38.
[32] C.I. Buba, S.E. Okhale, I. Muazzam, Garcinia kola: The phytochemistry, pharmacology and therapeutic applications, Int. J. Pharmacogn. 3 (2016) 67–81.
[33] T. Ogunmoyole, O. Olalekan, O. Fatai, J. Makun, I. Kade, Antioxidant and phytochemical profile of aqueous and ethanolic extract of *Garcinia kola*, J. Pharmacogn. Phytother. 4 (2012) 66–74.
[34] M. Farahna, P.F.S. Etet, S.Y. Osman, K.K. Yurt, N. Amir, L. Vecchio, I. Aydin, Y. H. Aldebasi, A. Sheikh, J.C. Chijuka, *Garcinia kola* aqueous suspension prevents cerebellar neurodegeneration in long-term diabetic rat–a type 1 diabetes mellitus model, J. Ethnopharmacol. 195 (2017) 159–165.
[35] E.O. Farombi, Bitter kola (Garcinia kola) seeds and hepatoprotection, in: Nuts and seeds in health and disease prevention, Elsevier, 2011, pp. 221–228.
[36] O.O. Igado, J.O. Olopade, A. Adesida, O.O. Aina, E.O. Farombi, Morphological and biochemical investigation into the possible neuroprotective effects of kolaviron

(*Garcinia kola* bioflavonoid) on the brains of rats exposed to vanadium, Drug Chem. Toxicol. 35 (2012) 371–380.
[37] F.F. Adekunle, F.A. Similoluwa, A.S. Adewale, Investigation of the effectiveness of biosynthesised gold nanoparticle from *Garcinia kola* leaves against fungal infections, Int. J. Nanopart. 12 (2020) 316–326.
[38] S.A. Akintelu, S.C. Olugbeko, A.S. Folorunso, Green synthesis, characterization, and antifungal activity of synthesized silver nanoparticles (AgNPS) from *Garcinia kola* pulp extract, BioNanoScience 12 (2022) 105–115.
[39] A. Sofowora, Medicinal plants and traditional medicine in Africa, John Wiley and sons LTD, 1982.
[40] G. Trease, W. Evans, A textbook of Pharmacognosy, Lond., BailliareTindall 12 (1983) 336.
[41] T.I. Borokini, F.O. Omotayo, Phytochemical and ethnobotanical study of some selected medicinal plants from Nigeria, J. Med. Plants Res. 6 (2012) 1106–1118.
[42] A. Akinsiku, Green synthesis of capped silver nanoparticles and their hybrids: Antimicrobial and optical properties, in, Covenant University, Ota, Nigeria., 2017.
[43] M. Składanowski, P. Golinska, K. Rudnicka, H. Dahm, M. Rai, Evaluation of cytotoxicity, immune compatibility and antibacterial activity of biogenic silver nanoparticles, Med. Microbiol. Immunol. 205 (2016) 603–613.
[44] J. Stetefeld, S.A. McKenna, T.R. Patel, Dynamic light scattering: a practical guide and applications in biomedical sciences, Biophys. Rev. 8 (2016) 409–427.
[45] U.K. Parida, S.K. Biswal, B.K. Bindhani, Green synthesis and characterization of gold nanoparticles: study of its biological mechanism in human SUDHL-4 cell line, Adv. Biol. Chem. 4 (2014) 360.
[46] O.B. Adewale, A. Onasanya, A.O. Fadaka, H. Iwere, S.O. Anadozie, O.A. Osukoya, I. I. Olayide, *In vitro* antioxidant effect of aqueous extract of *Solanum macrocarpon* leaves in rat liver and brain, Oxid. Antioxid. Med. Sci. 3 (2014) 225–229.
[47] I.F. Benzie, J.J. Strain, The ferric reducing ability of plasma (FRAP) as a measure of "antioxidant power": the FRAP assay, Anal. Biochem. 239 (1996) 70–76.
[48] T. Mosmann, Rapid colorimetric assay for cellular growth and survival: application to proliferation and cytotoxicity assays, J. Immunol. Methods 65 (1983) 55–63.
[49] A.A. Baharuddin, R.A.J. Roosli, Z.A. Zakaria, S.F.Md Tohid, Dicranopteris linearis extract inhibits the proliferation of human breast cancer cell line (MDA-MB-231) via induction of S-phase arrest and apoptosis, Pharm. Biol. 56 (2018) 422–432.
[50] J. Santhoshkumar, S. Rajeshkumar, S. Venkat, Kumar, Phyto-assisted synthesis, characterization and applications of gold nanoparticles - A review, Biochem. Biophys. Rep. 11 (2017) 46–57.
[51] D.G. Sant, T.R. Gujarathi, S.R. Harne, S. Ghosh, R. Kitture, S. Kale, B.A. Chopade, K.R. Pardesi, *Adiantum philippense* L. Frond assisted rapid green synthesis of gold and silver nanoparticles, J. Nanopart. 2013 (2013), 182320.
[52] D. Baruah, M. Goswami, R.N.S. Yadav, A. Yadav, A.M. Das, Biogenic synthesis of gold nanoparticles and their application in photocatalytic degradation of toxic dyes, J. Photochem. Photobiol. B: Biol. 186 (2018) 51–58.
[53] S. Ghosh, S. Patil, M. Ahire, R. Kitture, D.D. Gurav, A.M. Jabgunde, S. Kale, K. Pardesi, V. Shinde, J. Bellare, D.D. Dhavale, B.A. Chopade, *Gnidia glauca* flower extract mediated synthesis of gold nanoparticles and evaluation of its chemocatalytic potential, J. Nanobiotechnology 10 (2012) 17.
[54] T. Muthukumar, Sudhakumari, B. Sambandam, A. Aravinthan, T.P. Sastry, J.-H. Kim, Green synthesis of gold nanoparticles and their enhanced synergistic antitumor activity using HepG2 and MCF7 cells and its antibacterial effects, Process Biochem. 51 (2016) 384–391.
[55] S. Khorrami, A. Zarrabi, M. Khaleghi, M. Danaei, M.R. Mozafari, Selective cytotoxicity of green synthesized silver nanoparticles against the MCF-7 tumor cell line and their enhanced antioxidant and antimicrobial properties, Int. J. Nanomed. 13 (2018) 8013–8024.
[56] E. Joseph, G. Singhvi, - Multifunctional nanocrystals for cancer therapy: a potential nanocarrier, in: A.M. Grumezescu (Ed.), Nanomaterials for Drug Delivery and Therapy, William Andrew Publishing, 2019, pp. 91–116.
[57] J. Spadavecchia, D. Movia, C. Moore, C.M. Maguire, H. Moustaoui, S. Casale, Y. Volkov, A. Prina-Mello, Targeted polyethylene glycol gold nanoparticles for the treatment of pancreatic cancer: from synthesis to proof-of-concept in vitro studies, Int. J. Nanomed. 11 (2016) 791.
[58] M. Irfan, T. Ahmad, M. Moniruzzaman, S. Bhattacharjee, B. Abdullah, Size and stability modulation of ionic liquid functionalized gold nanoparticles synthesized using *Elaeis guineensis* (oil palm) kernel extract, Arab. J. Chem. 13 (2020) 75–85.
[59] S. Singh, D. Singh, M. Singh, Synthesis of nanostructured thin films for resolution and diffraction/camera length calibration of transmission electron microscopes, Indian J. Pure Appl. Phys. (IJPAP) 57 (2019) 157–165.
[60] M.A. Asadabad, M.J. Eskandari, Electron diffraction, Modern Electron Microscopy in Physical and Life Sciences, (2016).
[61] R. Karthik, K. Saravanakumar, S.-M. Chen, J.V. Kumar, C.-M. Lee, B.-S. Lou, V. Muthuraj, A. Elangovan, S. Kulandaivel, Eco-friendly synthesis of gold nanoparticles by using *B. javanica* blume leaves extract encapsulated with graphene oxide for selective electrochemical detection of dopamine, Int. J. Electrochem. Sci. 12 (2017) 1474–1491.
[62] A. Dzimitrowicz, P. Jamróz, I. Sergiel, T. Kozlecki, P. Pohl, Preparation and characterization of gold nanoparticles prepared with aqueous extracts of Lamiaceae plants and the effect of follow-up treatment with atmospheric pressure glow microdischarge, Arab. J. Chem. 12 (2019) 4118–4130.
[63] N.Y. Stozhko, M.A. Bukharinova, E.I. Khamzina, A.V. Tarasov, M.B. Vidrevich, K. Z. Brainina, The effect of the antioxidant activity of plant extracts on the properties of gold nanoparticles, Nanomater. (Basel) 9 (2019) 1655.
[64] J.R. Nakkala, R. Mata, S.R. Sadras, The antioxidant and catalytic activities of green synthesized gold nanoparticles from *Piper longum* fruit extract, Process Saf. Environ. Prot. 100 (2016) 288–294.
[65] O.Z. Olatunde, D. Tian, J. Yong, C. Lu, Chemical compositions of the essential oil extracted from the seeds of *Garcina kola*, and its biological activities, *Biomedical and Pharmacology*, Journal 14 (2021) 607–621.
[66] Y.J. Lee, E.-Y. Ahn, Y. Park, Shape-dependent cytotoxicity and cellular uptake of gold nanoparticles synthesized using green tea extract, Nanoscale Res. Lett. 14 (2019), 129-129.